International Symposium
On Turbulence and Shear Flow
Phenomena (TSFP-9)
June 30 - July 3, 2015 *Melbourne, Australia*

A-PRIORI ANALYSIS OF A LES MODEL FOR SCALAR FLUX BASED ON INTERSCALE ENERGY TRANSFER

Markus Klein, Christoph Wolff, Eike Tangermann
Fakultät für Luft- und Raumfahrttechnik, Universität der Bundeswehr München,
Werner-Heisenberg-Weg 39, 85577 Neubiberg, Germany
markus.klein@unibw.de

ABSTRACT

Fluid mixing by turbulent motion occurs in many technical devices and has a strong impact on mass transfer, heat-transfer and chemical reaction (see e.g. Peng and Davidson (2002), Younis et al. (2005), Rossi (2010)). In Large Eddy Simulation (LES) the turbulent subgrid flux has to be modeled. Many simulations for heat or mass transfer rely on the classical linear eddy diffusivity approach which is in many cases not appropriate. As an example Fig.1 shows that even the simple plane jet shear flow considered in this work features counter-gradient transport. Similar to momentum transport in LES, the scale similarity model for SGS scalar flux is known to correlate well with the stresses evaluated from DNS (Peng and Davidson (2002)). However the model does not provide enough dissipation. Recently Anderson and Domaradzki (2012) analysed the interscale energy transfer of the scale similarity model in the context of momentum transport and, based on the results, proposed a new SGS model. In the present work this model will be modified to account for LES scalar fluxes. It will be analysed a-priori using a newly generated plane jet DNS database at Re=10000.

(a)

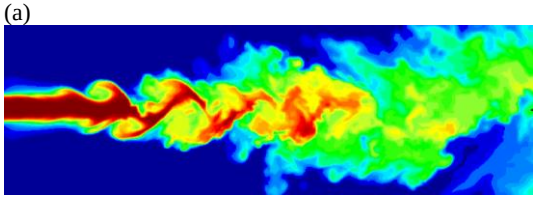

(b)

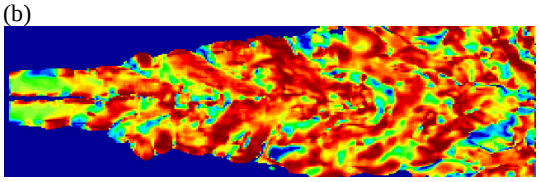

Figure 1. Instantaneous views of the jet flow. (a) Passive scalar distribution. (b) Cosine of the angle between the vectors $-\nabla \bar{f}$ and $\overline{uf} - \bar{u}\bar{f}$. Brown color indicates a value of 1 and blue color a value of -1.

PLANE JET DNS DATABASE

For the a-priori analysis performed in this work a turbulent plane jet is simulated for a Reynolds number $Re = (U_0 D)/\nu$ of 10000 where U_0 denotes the bulk velocity, D the nozzle diameter and ν the kinematic viscosity. The incompressible Navier-Stokes equations are solved together with the transport equation for a passive scalar on a staggered grid. A finite volume technique with 2nd order central differences and a 3rd order Runge Kutta time advancement are used.

The computational domain spans 20D in axial (x), 6.4D in homogenous (y) and 20D in lateral direction (z). The domain is resolved with 1200×256×1000=307.2· 10^6 grid points. The nozzle is resolved with 80 cells and the grid is stretched towards the lateral boundaries (see Fig. 2).

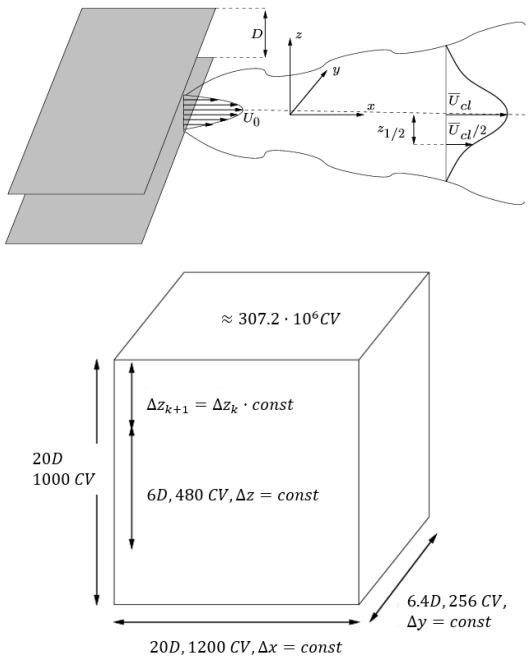

Figure 2. Sketch of the flow (top) and the computational domain (bottom).

The turbulent inflow data is generated using filtered random data. Further details on the numerical scheme, the configuration (at a lower Reynolds number) and the boundary conditions are given in Klein et al. (2003a, 2003b).

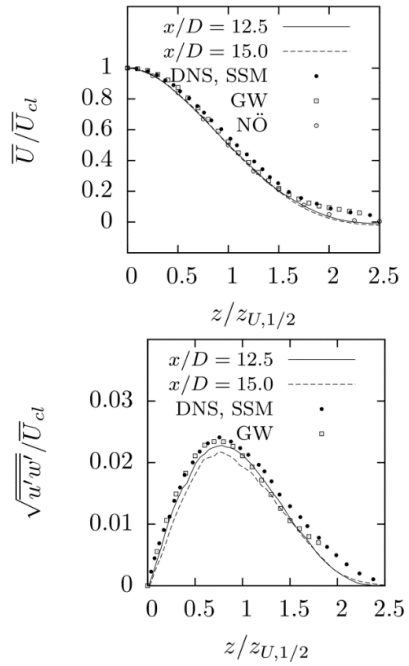

Figure 3: Mean axial velocity (top) and shear stress (bottom) normalized with the centerline velocity U_{cl} plotted in spanwise direction, normalized with the jet half width $z_{U,1/2}$.

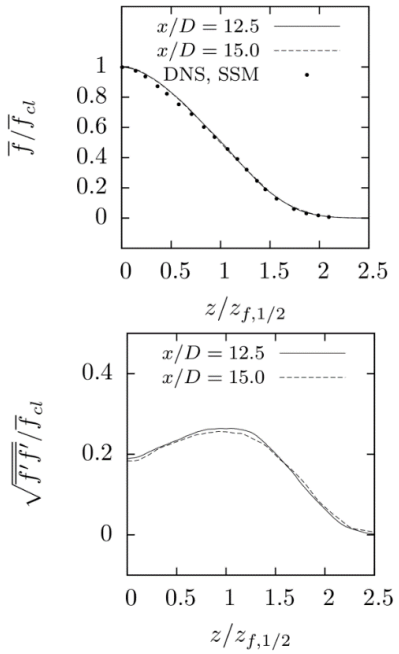

Figure 4: Mean scalar profiles (top) and fluctuations (bottom) normalized with the centerline value f_{cl} plotted in spanwise direction, normalized with the jet half width $z_{f,1/2}$.

Figures 3 and 4 show selected self-similar profiles at two different axial locations together with available experimental (Gutmark and Wygnansky 1976 (GW), Namer and Ötügen 1988 (NÖ)) or DNS data (Stanley et al. 2002 (SSM)) in order to demonstrate the accuracy of the DNS solution.

MODEL FORMULATION

In order to derive the model the scalar and turbulent kinetic energy spectrum is, following Anderson and Domaradzki, split in 3 different regions denoting smallest R_3 , intermediate R_2 and large scales R_1 (see Fig. 5). R_3 represents the scales unresolved by the mesh. Consequently the passive scalar is split into $f = f^1 + f^2 + f^3$ and the same decomposition is used for velocity. For each region the quantity f can be defined using two filtering levels such that f^1 can be represented by $\hat{\bar{f}}$, f^2 by $\bar{f} - \hat{\bar{f}}$ and f^3 by $f - \bar{f}$.

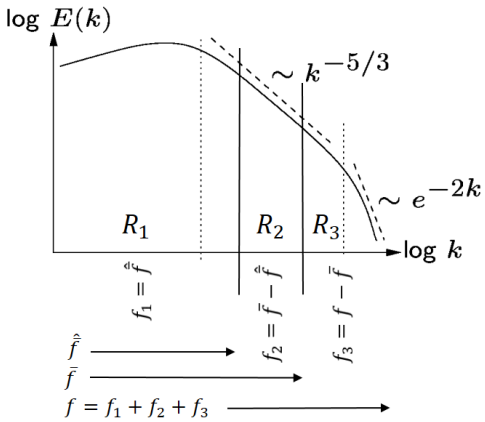

Figure 5: Sketch of the energy spectrum and its decomposition into different regions.

The product $u_i^l f^k$ of the individual contributions can again be attributed to a scale range m and the resulting expression is denoted N_i^{lkm}. Information for range R^3 is not available and the idea of the model is to remove the key production terms in range R^2. This results, following the original work, in the following model expression

$$\tau_j \coloneqq \overline{u_j f} - \overline{u}_j\ \bar{f} \approx -N_j^{112} - N_j^{122} = -\left(\hat{\bar{f}}\widehat{\bar{u}_j} - \hat{\bar{f}}\widehat{\bar{u}_j}\right) - \left(\hat{\bar{f}}\,\overline{u_j}' - \hat{\bar{f}}\widehat{\overline{u_j}'}\right) \quad (1)$$

where $\overline{u_j}' \coloneqq \overline{u_j} - \widehat{\bar{u}_j}$. However this model is not Galilei invariant and has to be replaced with one of the following two expressions:

$$\tau_j^{\mathrm{ADM}} \approx -N_j^{112,*} - N_j^{122} = -\left(\hat{\bar{f}}\,\widehat{\bar{u}_j} - \hat{\bar{f}}\widehat{\bar{u}_j}\right) - \left(\hat{\bar{f}}\,\overline{u_j}' - \hat{\bar{f}}\widehat{\overline{u_j}'}\right) \quad (2)$$

$$\tau_j \approx -\left(\hat{\bar{f}}\,\overline{u}_j - \hat{\bar{f}}\widehat{\overline{u}_j}\right) \quad (3)$$

Details are for the sake of brevity omitted and the reader is referred to the work of Anderson and Domaradzki. The model given by eq. (2) wil henceforth be denoted ADM model. The model represented by eq. (3) did show very poor correlation performance. For all primary and secondary filter width investigated in this work the correlation coefficient was smaller than 0.15. Hence, despite its compact form, it will not

be considered further. Still another model can be proposed starting from $\tau_j \approx -N_j^{112} - N_j^{122} - N^{212}$ which is, after manipulating some of the terms also Galilei invariant:

$$\tau_j^{\mathrm{ADS}} \approx \widehat{\hat{f}\,\overline{u_j}} - \hat{\hat{f}}\,\widehat{\overline{u_j}} + \widehat{\overline{u_j}\,\hat{f}} - \hat{\hat{f}}\,\widehat{\overline{u_j}} \qquad (4)$$

The model will be denoted ADS model due to its symmetry with respect to the roles of f and u. It is interesting to note that, if the scalar variable f is replaced with the velocity component u_i and the expression is multiplied with density, a model for momentum transport is obtained which is symmetric and Galilei invariant even for compressible flows.

ANALYSIS AND RESULTS

For the purpose of the current analysis, the DNS data has been explicitly filtered using a Gaussian filter kernel of the form $G(r) = (6/\pi\Delta^2)^{3/2} \exp(-6\, r \cdot r\, /\Delta^2)$. Results will be presented for five different filter widths corresponding to $\Delta = 2\Delta_{\mathrm{DNS}}, 4\Delta_{\mathrm{DNS}}, 8\Delta_{\mathrm{DNS}}, 16\Delta_{\mathrm{DNS}}, 32\Delta_{\mathrm{DNS}}$ or in terms of nozzle diameter $\Delta = \mathrm{D}/20, \mathrm{D}/10, \mathrm{D}/5, \mathrm{D}/2.5$. The secondary filter is given by the expression

$$\hat{f}_{i,j,k} = \sum_{di,dj,dk=-1,1} a_{di} a_{dj} a_{dk} \cdot f_{i+di,j+dj,k+dk} \qquad (5)$$
$$(a_{d-1}, a_{d0}, a_{d1}) = (C, 1-2C, C)$$

where C is a free positive parameter with $C \leq 1/3$. Based on the analysis of channel flow LES data Anderson and Domaradzki suggest to use $C = 1/12$.

LES models need to accurately capture the local behavior of scalar flux components and hence the Pearson correlation coefficient is in this work considered an important indicator for the quality of scalar flux models and should be as close to unity as possible. Before comparing different models with each other the influence of the secondary filter width in the models ADM and ADS is investigated. Results are exemplarily shown for two primary filter widths i.e. $\Delta = 4\Delta_{\mathrm{DNS}}, 16\Delta_{\mathrm{DNS}}$ and four different parameters C of the secondary filter.

Table 1. Correlation between modelled scalar flux in axial direction using the ADM model (see eq. (2)) and the ADS model (see eq. (4)) and DNS flux for two primary filter widths and different filter parameters C.

	ADM		ADS	
C	$\frac{\Delta}{\Delta_{\mathrm{DNS}}} = 4$	$\frac{\Delta}{\Delta_{\mathrm{DNS}}} = 16$	$\frac{\Delta}{\Delta_{\mathrm{DNS}}} = 4$	$\frac{\Delta}{\Delta_{\mathrm{DNS}}} = 16$
1/6	0.15	0.15	0.80	0.70
1/12	0.30	0.29	0.82	0.72
1/24	0.52	0.50	0.82	0.71
1/48	0.71	0.64	0.82	0.70

Table 1 shows a relatively weak dependence of the correlation magnitude on the primary filter for the two filter widths considered here, in particular for the ADM model. However, it can be seen that there is a pronounced sensitivity of the correlation coefficient on the filter parameter C for the ADM model, whereas the ADS model is considerably less sensitive to the width of the secondary filter and seems to show the best results for $C = 1/12$. In order to investigate this behavior in more detail, Table 2 shows the ratio of the Euclidian length of the vectors $N_j^{112,*}$ and N_j^{122} in equation (2).

Table 2. Ratio of the Euclidian length of the vectors $N_j^{112,*}$ and N_j^{122} for two primary filter widths and different filter parameters C.

C	$\frac{\Delta}{\Delta_{\mathrm{DNS}}} = 4$	$\frac{\Delta}{\Delta_{\mathrm{DNS}}} = 16$
1/6	0.16	0.17
1/12	0.33	0.35
1/24	0.70	0.79
1/48	1.43	1.61

It can be clearly seen that $N_j^{112,*}$ dominates over N_j^{122} for small test filter width which can be understood from the fact that N_j^{122} contains the expression $\overline{u_j}' \coloneqq \overline{u_j} - \widehat{\overline{u_j}}$ which obviously approaches zero if region R_2 of the intermediate scales becomes more and more narrow. As a result of this, the model is dominated by the term $N_j^{112,*}$ which looks similar to a scale similarity model given by the expression below:

$$\tau_j^{\mathrm{SSM}} \approx \widehat{\hat{f}\,\overline{u_j}} - \hat{\hat{f}}\,\widehat{\overline{u_j}} \qquad (6)$$

For small values of C the second term $-N_j^{122}$, which according to Anderson and Domaradzki (2012) obviously results in an improved dissipation characteristic of the model, is prevalent. The correlation coefficient of the expression $-N_j^{112,*} - N_j^{122}$ approaches for decreasing values of C the correlation coefficients of the scale similarity model (SSM) which are shown in Table 3 but are always to some extend smaller.

Table 3. Correlation between modelled scalar flux in axial direction using SSM model (see eq. (6)) and DNS flux for two primary filter widths and different filter parameters C.

	SSM	
C	$\frac{\Delta}{\Delta_{\mathrm{DNS}}} = 4$	$\frac{\Delta}{\Delta_{\mathrm{DNS}}} = 16$
1/6	0.80	0.71
1/12	0.81	0.70
1/24	0.81	0.69
1/48	0.81	0.69

Table 3 also shows that the SSM model is not very sensitive to the second filter. In all results presented below we will therefore use the value $C = 1/12$ whenever the filter given by eq. (5) is used. It is important to keep in mind that the correlation coefficient for the ADM model will improve when a smaller C is used. However, since the model converges towards the SSM model in this case it is not required to show the results separately. Final assessment of the models and the

magnitude of the parameter C has to be done using a-posteriori analysis.
For comparison results for the ADM, ADS and SSM model will be shown together with those for the classical gradient flux approximation (GFM) using $C_s = 0.1, \quad Sc_t = 1.0$

$$\tau_j^{\mathrm{GFM}} \approx -\frac{\mu_t}{Sc_t}\frac{\partial \bar{f}}{\partial x_i}, \quad \mu_t = (C_s\Delta)^2\sqrt{2\,\overline{S_{ij}}\,\overline{S_{ij}}} \qquad (7)$$

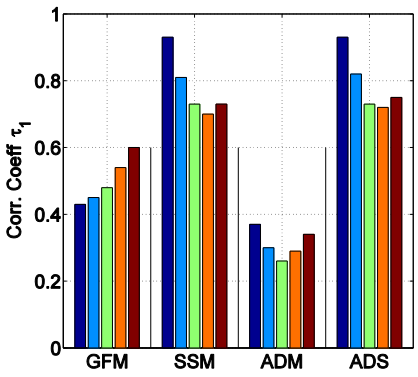

(a)

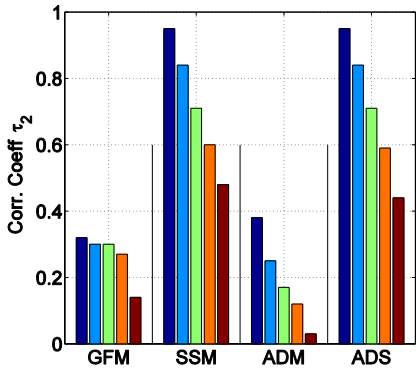

(b)

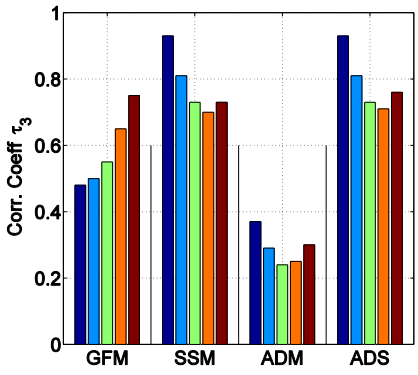

(c)

Figure 6: Correlation coefficient between $\tau_{l,Mod}$ and $\tau_{l,DNS}$ for the four different models for five different filter widths: $\Delta = 2\Delta_{\mathrm{DNS}}$ (■); $\Delta = 4\Delta_{\mathrm{DNS}}$ (■); $\Delta = 8\Delta_{\mathrm{DNS}}$ (■); $\Delta = 16\Delta_{\mathrm{DNS}}$ (■) and $\Delta = 32\Delta_{\mathrm{DNS}}$ (■); (a) x-direction; (b) y-direction; (c) z-direction.

The analysis of the subgrid scale models is in the following split into two parts. The correlation coefficient provides local information about the fluctuation and alignment of scalar flux and the corresponding model expression. If the correlation coefficients are calculated for each individual component of the scalar flux this will be denoted vector level analysis.

Fig. 6 shows the correlation coefficients for all models for five different filter widths. As expected, in general the correlation strength decreases with increasing filter width. An exception is the GFM model in τ_1, τ_3 direction. The ADM model shows overall low correlations for the chosen secondary filter. We note again that for smaller filter size the correlation strength would increase. However, since the model behavior approaches that of the SSM model in this case, these results are not shown separately. The GFM model performs in particular poor in direction τ_2 where the flow is statistically homogeneous. The best correlations are achieved by the SSM and ADS models even for relatively large filter size.

For passive scalar transport and under the assumption of local equilibrium the expression $\tau_i \partial \bar{f}/\partial x_i$ represents the subfilter dissipation rate (Fabre and Balarac (2011)). The corresponding analysis at the scalar level will give some information in regards of the dissipation characteristics of the model.

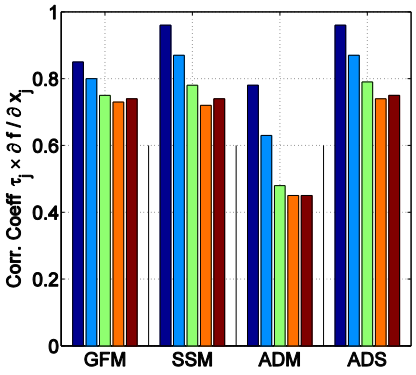

Figure 7: Correlation coefficient between $\tau_i \partial \bar{f}/\partial x_i$ calculated from the four different model expressions and DNS data for five different filter widths (legend as in Fig. 6).

Fig. 7 shows the correlation coefficients at the scalar level. The SSM and ADS model depict a performance similar to the vector level analysis. However, the GFM and ADM model show considerably stronger correlations, which might be an indication for their strength to represent dissipative effects.

The correlation is only a measure of linear dependence between two quantities and hence invariant under multiplication of the model with a constant. The second step

in the analysis is therefore to compare the magnitude of modelled scalar flux with the magnitude of its corresponding DNS value. Although eqs. (2),(4),(6) do not contain model constants it is possible to scale these models. In a-priori analysis the model coefficient can be determined conveniently using a least square approach. Eq. (8) results in a global model coefficient whereas eq. (9) gives a local approximation.

$$C_{\mathrm{Mod}} = \frac{\sum_{ijk}\sum_{l=1,2,3}\tau_{l,Mod}\times\tau_{l,DNS}}{\sum_{ijk}\sum_{l=1,2,3}\tau_{l,DNS}\times\tau_{l,DNS}} \qquad (8)$$

$$C_{\mathrm{Mod,loc}} = \frac{\sum_{l=1,2,3}\tau_{l,Mod}\times\tau_{l,DNS}}{\sum_{l=1,2,3}\tau_{l,DNS}\times\tau_{l,DNS}} \qquad (9)$$

Finally eq. (10) is used to measure the relative error between modeled scalar flux and the corresponding value evaluated from DNS.

$$\epsilon_{\mathrm{rel}} = \frac{\sum_{ijk}\sum_{l=1,2,3}\left|\tau_{l,Mod}-\tau_{l,DNS}\right|}{\sum_{ijk}\sum_{l=1,2,3}\left|\tau_{l,DNS}\right|} \qquad (10)$$

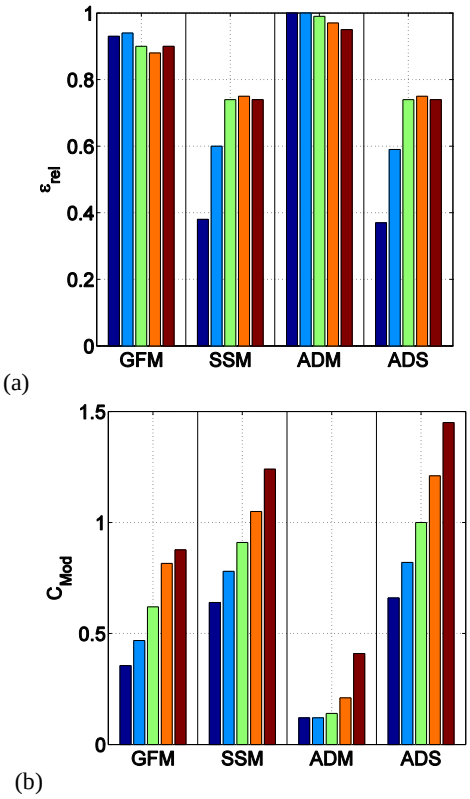

Figure 8: (a) Relative error ϵ_{rel} for the four different models after scaling them with global multipliers C_{mod} for five different filter widths: $\Delta = 2\Delta_{\mathrm{DNS}}$ (■); $\Delta = 4\Delta_{\mathrm{DNS}}$ (■); $\Delta = 8\Delta_{\mathrm{DNS}}$ (■);$\Delta = 16\Delta_{\mathrm{DNS}}$ (■) and $\Delta = 32\Delta_{\mathrm{DNS}}$(■); (b) Global model multipliers C_{mod} (see eq. (9)). Note that C_{GFM} is multiplied with 0.1.

Results for the relative error of the different models together with the optimal global multipliers are show in Figs 8 (a) and (b) respectively. As can be seen from Fig. 8 (b) the optimal multipliers increase with increasing filter width for all models. It is noted that the Smagorinsky constant was obviously chosen too small in the beginning which explains the upscaling (note the different scale for the GFM model in Fig 8 (b)). For the SSM and ADS model C_{SSM} and C_{ADS} are at the order of 1.0 whereas the ADM model seems to require a somewhat smaller model multiplier. The errors shown in Fig. 8 (a) are relatively large. The ADS model shows the smallest deviation to the DNS data but the difference to the SSM model is hardly visible.

Using the local multiplies according to eq. (9) the relative errors decrease remarkably as depicted in Fig 9 (a). The performance of the ADM model is now in between the GFM model and the models ADM and ADS. Whereas, the error of the GFM model is nearly independent of the filter width, the other errors approach zero for very small filter width.

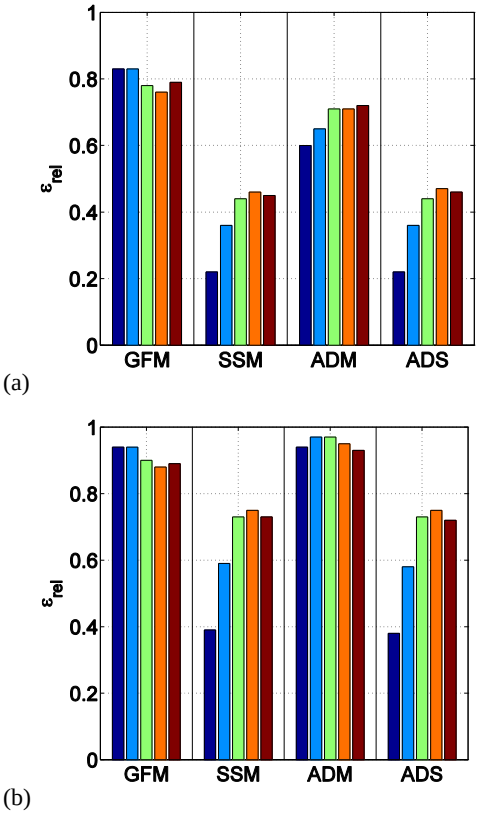

Figure 9: (a) Relative error ϵ_{rel} for the four different models after scaling them with local multipliers $C_{mod,loc}$ (see eq. (10)) for five different filter widths (legend as in Fig. 8). (b) Relative error ϵ_{rel} if $C_{mod,loc}$ is averaged in homogeneous direction (see eq. (11)).

Eqs. (8) and (9) cannot be used in a real LES. Instead a dynamic evaluation of the model parameter is required. The calculation of the model parameter typically requires a regularization in order to ensure the models good numerical properties. For this type of flow an averaging in the homogeneous y-direction is an obvious choice which results in a model parameter that is dependent on x and z-direction only:

$$C_{\mathrm{Mod,ik}} = \frac{\sum_j C_{\mathrm{Mod,loc}}(i,j,k)}{N_j} \qquad (12)$$

Comparing Fig. 9 (b) and Fig. 8 (a) shows however that the advantage of the local determination of the model parameter is lost after averaging in y-direction.

CONCLUSIONS

A direct numerical simulation of flow and mixing of a spatially developing plane jet at Re=10000 has been performed. The results show that the numerical scheme successfully captures the physics of this shear flow.

A new LES subgrid scale model for momentum transport, recently proposed by Anderson and Domaradzki (2012), has been modified to account for turbulent scalar SGS flux (ADM). Results indicate a pronounced sensitivity of the correlation strength on the width of the test filter. Anderson and Domaradzki demonstrated that their model shows considerable improvements compared with predictions of conventional scale similarity models. In particular the model is better suited to account for dissipative effects. Hence it is expected that there is a tradeoff between correlation strength observed in a-priori analysis and dissipation characteristics in a real LES. The model performance evaluated from a-priori analysis can be improved by choosing a smaller secondary filter width. In that case the ADM model approaches the behaviour of the SSM model. Furthermore a symmetric version of the ADM model has been suggested. The performance of this ADS model is very similar to the SSM model with very small advantages for the ADS model.

Final evaluation of the model performance has to come from a-posteriori analysis which is beyond the scope of this work but also part of the work in progress.

ACKNOWLEDGEMENTS

The author MK is thankful for many fruitful discussions with J. A. Domaradzki.

REFERENCES

B.W. Anderson and J.A. Domaradzki (2012). A sub-grid model for large eddy simulation based on the physics of interscale energy transfer in turbulence, Physics of Fluids, Vol. 24, 065104.

E. Gutmark and I. Wygnanski (1976). The planar turbulent jet. J. Fluid Mech., Vol. 73, pp.465-495.

Y. Fabre and G. Balarac, (2011). Development of a new dynamic procedure for the Clark model of the subgrid-scale scalar flux using the concept of optimal estimator, Physics of Fluids, Vol. 23, pp. 1 –11.

M. Klein, A. Sadiki and J. Janicka (2003a). A digital filter based generation of inflow data for spatially developing direct numerical or large eddy simula-tions. J. Comp. Physics, Vol. 186, pp.652-665.

M. Klein, A. Sadiki and J. Janicka (2003b). Investiga-tion of the Reynoldsnumber on a plane jet using direct numerical simulation. Int. J. of Heat and Fluid Flow, Vol. 24/61 pp.785-794.

I. Namer and M.V. Ötügen (1988). Velocity Meas-urements in a plane turbulent air jet at moderate Reynolds numbers. Experiments in Fluids, Vol. 6 pp.387-399.

S.H. Peng and L. Davidson (2002). On a subgrid scale heat flux model for large eddy simulation of turbulent thermal flow. Int. J. of Heat and Mass Trans., Vol. 55 pp.1393-1405,2002

R. Rossi (2010). A numerical study of algebraic flux models for heat and mass transport simulation in complex flows, International Journal of Heat and Mass Transfer, 53, 4511-4542.

P. Sagaut, (1998). Large Eddy Simulation for incompressible Flow, Springer Berlin Heidelberg.

S.A. Stanley, S. Sarkar and J.P. Mellado (2002). A study of the flow field evolution and mixing in a planar turbulent jet using direct numerical simulation. J. Fluid Mech., Vol. 450, pp. 377-407.

B.A. Younis, C.G. Speziale and T.T. Clark (2005). A rational model for the turbulent scalar fluxes, Proc. R. Soc. A, 461, pp. 575-594.